

Association of Presynaptic Loss with Alzheimer's Disease and Cognitive Decline

Guoyu Lan, PhD,^{1,2} Yue Cai, PhD,^{1,2} Anqi Li, MSc,¹ Zhen Liu, PhD,¹ Shaohua Ma, PhD,² and Tengfei Guo, PhD,^{1,3} for the Alzheimer's Disease Neuroimaging Initiative[†]

Objective: Increased presynaptic dysfunction measured by cerebrospinal fluid (CSF) growth-associated protein-43 (GAP43) may be observed in Alzheimer's disease (AD), but how CSF GAP43 increases relate to AD-core pathologies, neurodegeneration, and cognitive decline in AD requires further investigation.

Methods: We analyzed 731 older adults with baseline β -amyloid ($A\beta$) positron emission tomography (PET), CSF GAP43, CSF phosphorylated tau₁₈₁ (p-Tau₁₈₁), and ¹⁸F-fluorodeoxyglucose PET, and longitudinal residual hippocampal volume and cognitive assessments. Among them, 377 individuals had longitudinal ¹⁸F-fluorodeoxyglucose PET, and 326 individuals had simultaneous longitudinal CSF GAP43, $A\beta$ PET, and CSF p-Tau₁₈₁ data. We compared baseline and slopes of CSF GAP43 among different stages of AD, as well as their associations with $A\beta$ PET, CSF p-Tau₁₈₁, residual hippocampal volume, ¹⁸F-fluorodeoxyglucose PET, and cognition cross-sectionally and longitudinally.

Results: Regardless of $A\beta$ positivity and clinical diagnosis, CSF p-Tau₁₈₁-positive individuals showed higher CSF GAP43 concentrations ($p < 0.001$) and faster rates of CSF GAP43 increases ($p < 0.001$) compared with the CSF p-Tau₁₈₁-negative individuals. Moreover, higher CSF GAP43 concentrations and faster rates of CSF GAP43 increases were strongly related to CSF p-Tau₁₈₁ independent of $A\beta$ PET. They were related to more rapid hippocampal atrophy, hypometabolism, and cognitive decline ($p < 0.001$), and predicted the progression from MCI to dementia (area under the curve for baseline 0.704; area under the curve for slope 0.717) over a median 4 years of follow up.

Interpretation: Tau aggregations rather than $A\beta$ plaques primarily drive presynaptic dysfunction measured by CSF GAP43, which may lead to sequential neurodegeneration and cognitive impairment in AD or neurodegenerative diseases.

ANN NEUROL 2022;92:1001–1015

Introduction

The aggregation of extracellular β -amyloid ($A\beta$) plaques and intraneuronal neurofibrillary tau tangles are the two key hallmarks of Alzheimer's disease (AD),¹ which can be detected directly by positron emission tomography (PET) imaging^{2, 3} or indirectly by CSF $A\beta_{42}/A\beta_{40}$ ratio and phosphorylated tau (p-Tau) biomarkers.^{4, 5} According to the biological definition of AD⁶ and recent reports,^{7–10} $A\beta$ (A) pathology presents initially in disease onset,

followed by tau (T) aggregation, which subsequently results in neurodegeneration (N) and cognitive decline. However, several recent studies^{11–13} also identified different A/T/N profiles with overlapping features of neurodegeneration and cognitive decline, indicating we may need extra techniques beyond A/T/N biomarkers to understand the progression of the disease fully.¹⁴

Synaptic impairment appears closely linked to neurodegeneration and cognitive decline in AD.^{15–17} One

View this article online at wileyonlinelibrary.com. DOI: 10.1002/ana.26492

Received Jun 6, 2022, and in revised form Aug 22, 2022. Accepted for publication Aug 24, 2022.

Address correspondence to Dr Tengfei Guo, Institute of Biomedical Engineering, Shenzhen Bay Laboratory, No.5 Kelian Road, Shenzhen, 518132, China.
E-mail: tengfei.guo@szbl.ac.cn

[†]Data used in preparation of this article were obtained from the Alzheimer's Disease Neuroimaging Initiative (ADNI) database (adni.loni.usc.edu). As such, the investigators within the ADNI contributed to the design and implementation of ADNI and/or provided data, but did not participate in analysis or writing of this report. A complete listing of ADNI investigators can be found at: http://adni.loni.usc.edu/wp-content/uploads/how_to_apply/ADNI_Acknowledgement_List.pdf.

From the ¹Institute of Biomedical Engineering, Shenzhen Bay Laboratory, Shenzhen, China; ²Tsinghua Shenzhen International Graduate School (SIGS), Tsinghua University, Shenzhen, China; and ³Institute of Biomedical Engineering, Peking University Shenzhen Graduate School, Shenzhen, China

meta-analysis study¹⁶ suggested presynaptic markers may be affected more than postsynaptic markers in AD. Growth-associated protein-43 (GAP43) is a presynaptic membrane protein primarily expressed in the hippocampus and associated cortex, and participates in the regulation of synaptogenesis, synaptic plasticity, and axon outgrowth in the adult brain.^{18, 19} Post-mortem studies showed an apparent decrease in GAP43 expression in the frontal cortex and some hippocampal areas of AD brains.^{20, 21} At the same time, emerging evidence proved that CSF GAP43 concentrations increased in AD, but not in other neurodegenerative disorders.^{22, 23} However, two recent cross-sectional studies^{24, 25} reported conflicting findings about the associations among A β , tau, and CSF GAP43 dysfunction in AD. Specifically, the former²⁴ did not observe a significant difference between A+ /T- and A-/T- in individuals with mild cognitive impairment (MCI), whereas the latter²⁵ found elevated CSF GAP43 concentrations in A+ /T- group compared with the A-/T-group among cognitively unimpaired (CU) individuals. Consequently, the mechanism of GAP43 dysfunction during AD pathogenesis remains elusive.

In the present study, we compared CSF GAP43 among different clinical (CU, MCI, and dementia) and biological (A/T) stages of AD using both cross-sectional and longitudinal data from the Alzheimer's Disease Neuroimaging Initiative (ADNI) cohort. We also investigated the cross-sectional and longitudinal associations of CSF GAP43 with A β , tau, neurodegeneration, and cognitive decline in different A β positivity and clinical stages. We aimed to investigate the alterations of CSF GAP43 among different stages of AD, the associations of A β and tau pathologies with CSF GAP43, and the prediction of CSF GAP43 on longitudinal neurodegeneration and cognitive decline. The ultimate goal is to help understand the mechanisms underlying presynaptic loss, and how synaptic dysfunction results in neurodegeneration and cognitive decline in AD.

Methods

Participants

Data used in the preparation of this article were obtained from the ADNI database (adni.loni.usc.edu). The ADNI was launched in 2003 as a public-private partnership, led by Principal Investigator Michael W. Weiner, MD. The primary goal of ADNI is to test whether serial magnetic resonance imaging (MRI), PET, other biological markers, and clinical and neuropsychological assessment can be combined to measure the progression of MCI and early AD. The ADNI study was approved by the institutional review boards of all participating centers, and written

informed consent was obtained from all participants or their authorized representatives.

We identified 731 participants (232 CU, 395 MCI, and 104 dementia) with baseline ¹⁸F-florbetapir (FBP) A β PET and concurrent (within 1 year) CSF GAP43, CSF p-Tau₁₈₁, and ¹⁸F-fluorodeoxyglucose (FDG) PET, as well as longitudinal structure MRI (median 2.0 years, [interquartile range (IQR) 3.1 years of follow-up] and cognitive assessments (median 4.0 years [IQR 5.0 years] of follow up). Among them, 377 individuals had longitudinal FDG PET (median 2.0 years [IQR 2.4 years] of follow up), and 326 individuals had simultaneous longitudinal CSF GAP43, A β PET, and CSF p-Tau₁₈₁ data. In addition, 233 individuals had concurrent longitudinal CSF GAP43, A β PET, CSF p-Tau₁₈₁, and FDG PET data.

CSF Biomarkers

CSF GAP43 was detected by an in-house enzyme-linked immunosorbent assay method at the Clinical Neurochemistry Laboratory of the Sahlgrenska University Hospital (Möln达尔, Sweden), as described previously.²² CSF p-Tau₁₈₁ was analyzed by the ADNI biomarker core group using the fully automated Roche Elecsys.²⁶ The threshold of CSF p-Tau₁₈₁ positivity (T+) was defined as $\geq 23\text{pg/ml}$ according to the receiver operating characteristic analysis using the Youden index, classifying 326 A β - ADNI CU participants and 467 A β + ADNI MCI and dementia patients as the end-point (area under the curve [AUC] 0.86, 95% confidence interval [95% CI] 0.84–0.89). Linear mixed effect (LME) models were used to calculate slopes of CSF GAP43 (Δ CSF GAP43) and CSF p-Tau₁₈₁ (Δ CSF p-Tau₁₈₁) for all the participants with longitudinal CSF data, adjusting for age and sex, and including a random slope and intercept.

PET and MRI Imaging Processing

FBP PET and FDG PET data were acquired from 50 to 70 min (FBP, 4 \times 5-min frames) and 30–60 min (FDG, 6 \times 5-min frames) post-injection. PET images were motion corrected, time-averaged, and summed into one static frame, and more details are given elsewhere (<http://adni-info.org>).

FBP image was coregistered to their corresponding structural MRI scan that was closest in time to the PET scan. Cortical florbetapir uptake in 68 FreeSurfer-defined regions of interest defined by the Desikan–Killiany atlas²⁷ were extracted using FreeSurfer (v7.1.1). A cortical summary composite standardized uptake value ratio (SUVR) was calculated by referring FBP uptake in AD summarized cortical regions (including frontal, cingulate, parietal, and temporal regions) to the mean uptake of the whole cerebellum.²⁸ The A β + of FBP PET was defined as composite

SUVR ≥ 1.11 .²⁸ SUVRs that referred to one composite reference region (made up of the brainstem, whole cerebellum, and eroded white matter)²⁸ were used to calculate slopes of FBP SUVR ($\Delta A\beta$ PET) for all the participants with longitudinal FBP PET data using LME models, adjusting for age and sex, and including a random slope and intercept.

FDG images were spatially normalized in SPM12 to the MNI PET template. FDG SUVR in a pre-defined MetaROIs (made up of left angular gyrus, right angular gyrus, bilateral posterior cingulate, left inferior temporal gyrus, and right inferior temporal gyrus) were calculated by normalizing averaging FDG counts in MetaROIs to that found in the upper 50% of voxels in a pons/vermis reference region.²⁹ Slopes of FDG SUVR (Δ FDG PET) were calculated for all the participants with longitudinal FDG PET data using LME models, adjusting for age and sex, and including a random slope and intercept.

Hippocampal volume (HCV; cm³) was computed across hemispheres from the structural MRI scan via FreeSurfer, and adjusted by the estimated intracranial volume using the approach reported by Jack et al.³⁰ The residual HCV (rHCV) was calculated as the difference between the raw and expected HCV, as we described previously.⁸ Slopes of rHCV (Δ rHCV) were calculated for all the participants with longitudinal MRI data using LME models, adjusting for age and sex, and including a random slope and intercept.

Biological Stages Defined by A/T Biomarkers

Participants were classified into four different A/T profiles according to the abnormal status of $A\beta$ PET ($A\pm$) and CSF p-Tau₁₈₁ ($T\pm$) defined by the cut-off values as described above. For sensitivity analysis, we also used an alternative cut-off for CSF p-Tau₁₈₁ ≥ 19.2 pg/ml³¹ reported by a different cohort to define $T\pm$.

Cognitive Assessments

Previously validated preclinical Alzheimer cognitive composite (PACC)³² scores were used to represent global cognition. Briefly, PACC scores were computed by combining z-scores of several cognitive tests, including the delayed recall portion of the Alzheimer's Disease Assessment Scale, the delayed recall score on the logical memory IIa subtest from the Wechsler Memory Scale, the digit symbol substitution test score from the Wechsler Adult Intelligence Scale-Revised, and the Mini-Mental State Examination total score as described previously.⁸ Slopes of PACC scores (Δ PACC scores) were calculated for all the participants with longitudinal PACC data using LME models, adjusting for age, sex and education, and including a random slope and intercept.

Statistical Analysis

All statistical analyses were performed using R version 4.1.1 (The R Foundation for Statistical Computing, Vienna, Austria). Due to the limited sample size of dementia patients in some subsets, we combined MCI and dementia into the cognitively impaired (CI) group in our primary analysis. Data are presented as the median (IQR) or number (%), unless otherwise noted. A two-tailed significance level of $p < 0.05$ was applied if not otherwise stated. The characteristics at baseline of $A\beta-$ CU, $A\beta-$ CI, $A\beta+$ CU, and $A\beta+$ CI groups were compared by using a two-tailed Mann–Whitney U test or Fisher's exact test. A false discovery rate (FDR) of 0.05 was applied using the Benjamini–Hochberg approach for multiple comparisons correction.

We used generalized linear models to determine the associations of baseline CSF GAP43 and Δ CSF GAP43 with age, sex, and *APOE-e4* status. Generalized linear models were also used to compare baseline CSF GAP43 and Δ CSF GAP43 among clinical groups, $A\beta$ positivity/clinical groups, and A/T groups, controlling for age, sex, and *APOE-e4* status Benjamini–Hochberg's approach was used for multiple comparisons correction (FDR < 0.05).

To further explore the independent influence of $A\beta$ and tau pathologies on CSF GAP43, we subsequently investigated the prediction of baseline CSF GAP43 and Δ CSF GAP43 by including $A\beta$ PET and CSF p-Tau₁₈₁ as the predictors in one multivariate model in $A\beta-$ CU, $A\beta-$ CI, $A\beta+$ CU, and $A\beta+$ CI groups separately, controlling for the same covariates above.

To determine the predictive effect of CSF GAP43 on the disease progression, we used generalized linear models to investigate the associations of baseline CSF GAP43 and Δ CSF GAP43 with Δ rHCV, Δ FDG PET, and Δ PACC scores, controlling for the same covariates above. Additionally, we conducted a receiver operating characteristic curve analysis to investigate whether CSF GAP43 can predict the conversion from MCI to dementia at follow up. Finally, mediation analysis (R; Lavaan package)³³ was conducted to explore the sequential associations among longitudinal changes of CSF p-Tau₁₈₁, CSF GAP43, rHCV, and PACC scores.

Results

Demographics

The characteristics at baseline of participants are summarized in Table . Among 731 participants, 347 (48%) were women, 398 (54%) were *APOE-e4* carriers, 393 (54%) were $A\beta$ positive, and 499 (68%) were CI and the median age was 72.6 years (IQR 10.3 years). Longitudinal data of CSF GAP43, $A\beta$ PET, CSF p-Tau₁₈₁, rHCV, FDG PET,

TABLE. Demographics of Participants

Characteristic at baseline	A β - CU	A β - CI	A β + CU	A β + CI
No. patients (%)	154 (21)	184 (25)	78 (11)	315 (43)
Age (years)	71.5 (8.6)	69.8 (12.2)	75.2 (9.0) ^{a,b}	73.7 (9.8) ^{b,d,f}
Female, n (%)	75 (49)	82 (45)	53 (68) ^{d,e}	137 (43) ^c
Education, years	17 (2.8)	16 (4.0) ^d	16 (4.0) ^d	16 (4.0) ^a
CSF p-Tau ₁₈₁ positive, n (%)	37 (24)	40 (22)	41 (53) ^{a,b}	242 (77) ^{a,b,c}
APOE-e4 carriers, n (%)	33 (21)	46 (25)	33 (42) ^{a,e}	221 (70) ^{a,b,c}
A β PET SUVR	1.02 (0.08)	1.01 (0.07)	1.29 (0.21) ^{a,b}	1.40 (0.26) ^{a,b,c}
CSF p-Tau ₁₈₁ (pg/ml)	17.7 (7.8)	17.7 (9.0)	24.1 (13.3) ^{a,b}	31.3 (18.4) ^{a,b,c}
CSF GAP43 (pg/ml)	4,096 (2809)	3,747 (2386)	4756 (3909) ^b	5243 (3998) ^{a,b}
rHCV (cm ³)	-0.02 (0.47)	-0.11 (0.68) ^d	-0.11 (0.51) ^d	-0.44 (0.62) ^{a,b,c}
FDG PET SUVR (MetaROIs)	1.30 (0.13)	1.27 (0.17) ^d	1.28 (0.19) ^d	1.16 (0.21) ^{a, b, c}
PACC scores	0.76 (3.44)	-3.42 (4.72) ^a	-0.31 (3.86) ^b	-9.28 (9.71) ^{a,b,c}
326 participants with concurrent longitudinal Aβ PET, CSF p-Tau₁₈₁, CSF GAP43, MRI, and PACC data				
No. patients (%)	83 (25)	81 (25)	44 (14)	118 (36)
Visits of CSF GAP43, median (IQR, range)	2.0 (1.0, 2–3)	2.0 (1.0, 2–4)	2.0 (1.0, 2–3)	2.0 (1.0, 2–3)
Duration of CSF GAP43, years, median (IQR, range)	2.0 (2.0, 1.3–4.3)	3.1 (2.0, 1.7–6.0)	2.2 (2.0, 1.9–5.0)	2.0 (2.0, 1.7–5.0)
Visits of A β PET, median (IQR, range)	3.0 (1.5, 2–6)	4.0 (2.0, 2–6)	3.0 (1.3, 2–5)	3.0 (1.0, 2–6)
Duration of A β PET, years, median (IQR, range)	5.9 (4.4, 1.9–10.0)	6.0 (4.0, 1.9–10.2)	5.0 (3.0, 1.9–9.0)	4.0 (3.1, 1.9–9.2)
Visits of CSF p-Tau ₁₈₁ , median (IQR, range)	2.0 (1.5, 2–5)	3.0 (2.0, 2–5)	3.0 (2.0, 2–5)	2.0 (1.0, 2–4)
Duration of CSF p-Tau ₁₈₁ , years, median (IQR, range)	2.4 (3.3, 1.5–8.5)	4.0 (4.3, 1.7–9.1)	4.0 (3.7, 1.9–8.6)	2.1 (2.0, 1.7–8.4)
Visits of MRI, median (IQR, range)	4.0 (2.0, 2–9)	5.0 (3.0, 2–12)	4.0 (2.0, 2–8)	5.0 (2.0, 2–11)
Duration of MRI, years, median (IQR, range)	2.1 (4.6, 0.4–10.2)	4.0 (6.0, 0.8–11.2)	2.3 (4.7, 0.2–8.1)	2.1 (3.0, 0.5–9.9)
Visits of PACC, median (IQR, range)	6.0 (2.0, 3–9)	8.0 (4.0, 3–13)	6.0 (2.0, 3–10)	6.0 (2.0, 4–12)
Duration of PACC, years, median (IQR, range)	6.5 (4.2, 1.9–10.5)	7.0 (4.5, 2.0–11.2)	5.8 (4.0, 2.0–9.9)	4.1 (2.5, 1.9–11.0)
233 participants with longitudinal FDG PET				
No. patients (%)	49 (21)	67 (29)	29 (12)	88 (38)
Visits of FDG PET, median (IQR, range)	2.0 (0, 2–3)	2.0 (1, 2–3)	2.0 (0, 2–3)	2.0 (0, 2–3)
Duration of FDG PET, years, median (IQR, range)	2.0 (0.1, 1.5–6.8)	3.2 (4.2, 1.9–8.2)	2.0 (0.1, 1.9–7.1)	2.0 (2.9, 1.9–7.5)

Abbreviations: APOE, apolipoprotein E; CI, cognitively impaired; CU, cognitively unimpaired; GAP43, growth-associated protein-43; IQR, interquartile range; MetaROIs, left angular gyrus, right angular gyrus, bilateral posterior cingulate, left inferior temporal gyrus, right inferior temporal gyrus; PACC, Preclinical Alzheimer Cognitive Composite; p-Tau₁₈₁, phosphorylated tau181; rHCV, residual hippocampal volume; SUVR, standard uptake value ratio. Data are presented as median (IQR) or number (%). Multiple comparisons correction was used (false discovery rate <0.05).

^ap <0.001 versus A β - CU.

^bp <0.001 versus A β - CI.

^cp <0.001 versus A β + CU.

^dp <0.05 versus A β - CU.

^ep <0.05 versus A β - CI.

^fp <0.05 versus A β + CU.

and PACC scores are also illustrated in Table . In the whole cohort, older ages were associated with higher baseline CSF GAP43 (standardized β [β_{std}] = 0.12 [95% CI 0.05–0.19], p = 0.001), but not with Δ CSF GAP43. *APOE-ε4* carriers had higher baseline CSF GAP43 (estimate = 1,089 [95% CI 0.24–0.53], p < 0.001) and faster Δ CSF GAP43 increases (estimate = 29 [95% CI 0.27–0.71], p < 0.001) than *APOE-ε4* non-carriers.

Comparison of CSF GAP43 among Different Clinical and Biological Stages of AD

At baseline, the dementia group had higher CSF GAP43 concentrations than the MCI group (estimate = 847 [95% CI 0.08–0.51], p = 0.007) and CU group (estimate = 965 [95% CI 0.10–0.57], p = 0.007; Fig 1A). After stratified by A β positivity, higher CSF GAP43 concentrations were found in A $\beta-$ dementia (estimate = 2,452 [95% CI 0.30–1.43], p = 0.005), A $\beta+$ MCI (estimate = 1,144 [95% CI 0.19–0.61], p < 0.001), and A $\beta+$ dementia (estimate = 1,273 [95% CI 0.18–0.71], p = 0.002), but not in A $\beta-$ MCI and A $\beta+$ CU groups compared with the A $\beta-$ CU individuals (Fig 1B). Longitudinally, only A $\beta+$ MCI individuals showed faster Δ CSF GAP43 increases (estimate = 31 [95% CI 0.22–0.82], p = 0.004) than the A $\beta-$ CU group (Fig 2B). Notably, we also observed marginally higher CSF GAP43 concentrations (estimate = 694 [95% CI –0.02 to 0.51], p = 0.079) in A $\beta+$ CU individuals than A $\beta-$ CU individuals.

To further explore the associations of CSF GAP43 with A β and tau pathologies, we compared cross-sectional and longitudinal CSF GAP43 among different A/T profiles. Notably, both A-/T+ and A+/T+ had significantly higher CSF GAP43 concentrations than the A-/T- and A+/T- groups regardless of clinical status (Fig 1C). Similar to baseline, significantly faster Δ CSF GAP43 increases were also found in A-/T+ and A+/T+ groups compared with the A-/T- and A+/T- groups (Fig 2C).

Additionally, the results were duplicated using the alternative cut-off for CSF p-Tau₁₈₁ to define tau-positivity (T±).

Association of CSF GAP43 with A β PET and CSF p-Tau₁₈₁

Regardless of A β and clinical status, higher CSF p-Tau₁₈₁ concentrations were related to greater baseline CSF GAP43 (A $\beta-$ CU: β_{std} = 0.72 [95% CI 0.61–0.84], p < 0.001; A $\beta-$ CI: β_{std} = 0.78 [95% CI 0.68–0.87], p < 0.001; A $\beta+$ CU: β_{std} = 0.66 [95% CI 0.48–0.84], p < 0.001; A $\beta+$ CI: β_{std} = 0.76 [95% CI 0.68–0.83], p < 0.001) and faster Δ CSF GAP43 increases (A $\beta-$ CU:

β_{std} = 0.73 [95% CI 0.57–0.88], p < 0.001; A $\beta-$ CI: β_{std} = 0.77 [95% CI 0.61–0.93], p < 0.001; A $\beta+$ CU: β_{std} = 0.75 [95% CI 0.52–0.97], p < 0.001; A $\beta+$ CI: β_{std} = 0.73 [95% CI 0.60–0.86], p < 0.001; Fig 3A–D). When additionally controlling for baseline CSF GAP43 concentrations, higher CSF p-Tau₁₈₁ concentrations were still related to faster Δ CSF GAP43 increases in A $\beta-$ CU (β_{std} = 0.16 [95% CI 0.04–0.28], p = 0.009), A $\beta-$ CI (β_{std} = 0.16 [95% CI 0.03–0.29], p = 0.019) and A $\beta+$ CU (β_{std} = 0.22 [95% CI 0.08–0.36], p = 0.002), but not in A $\beta+$ CI.

Moreover, Δ CSF p-Tau₁₈₁, but not Δ A β PET were positively associated with faster Δ CSF GAP43 increases in all subgroups (A $\beta-$ CU: β_{std} = 0.54 [95% CI 0.34–0.74], p < 0.001; A $\beta-$ CI: β_{std} = 0.47 [95% CI 0.24–0.69], p < 0.001; A $\beta+$ CU: β_{std} = 0.57 [95% CI 0.30–0.84], p < 0.001; A $\beta+$ CI: β_{std} = 0.50 [95% CI 0.34–0.66], p < 0.001; Fig 3E,F). Only in A $\beta+$ CI did the positive link (β_{std} = 0.16 [95% CI 0.10–0.22], p < 0.001) between Δ CSF p-Tau₁₈₁ and Δ CSF GAP43 persist after adjusting for baseline levels of A β PET, CSF p-Tau₁₈₁, and CSF GAP43.

Association of CSF GAP43 with Longitudinal Neurodegeneration and Cognitive Decline

In the whole cohort, higher baseline CSF GAP43 concentrations were associated with faster Δ rHCV decreases (Fig 4A; β_{std} = –0.15 [95% CI –0.22 to –0.08], p < 0.001) and Δ PACC scores decreases (Fig 4E; β_{std} = –0.19 [95% CI –0.26 to –0.12], p < 0.001). Likewise, faster Δ CSF GAP43 increases were also related to faster Δ rHCV decreases (Fig 4B; β_{std} = –0.23 [95% CI –0.33 to –0.12], p < 0.001) and Δ PACC scores decreases (Fig 4F; β_{std} = –0.19 [95% CI –0.29 to –0.08], p < 0.001). After stratified by A β and cognition status, higher baseline CSF GAP43 concentrations (β_{std} = –0.15 [95% CI –0.25 to –0.04], p = 0.008) and faster Δ CSF GAP43 increases (β_{std} = –0.25 [95% CI –0.42 to –0.07], p = 0.006) were related to faster Δ rHCV decreases only in A $\beta+$ CI. In addition, baseline CSF GAP43 concentrations, but not Δ CSF GAP43, were negatively associated with faster Δ PACC scores decreases in A $\beta-$ CI (β_{std} = –0.19 [95% CI –0.34 to –0.05], p = 0.008) and A $\beta+$ CI (β_{std} = –0.13 [95% CI –0.24 to –0.02], p = 0.019). In the subgroups of individuals with longitudinal FDG PET scan, both higher baseline CSF GAP43 (Fig 4C; β_{std} = –0.19 [95% CI –0.29 to –0.09], p < 0.001, n = 377) and faster Δ CSF GAP43 increases (Fig 4D; β_{std} = –0.19 [95% CI –0.32 to –0.06], p = 0.003, n = 233) were associated with faster Δ FDG PET decreases. When stratified by A β and cognition status, the link between baseline or longitudinal CSF

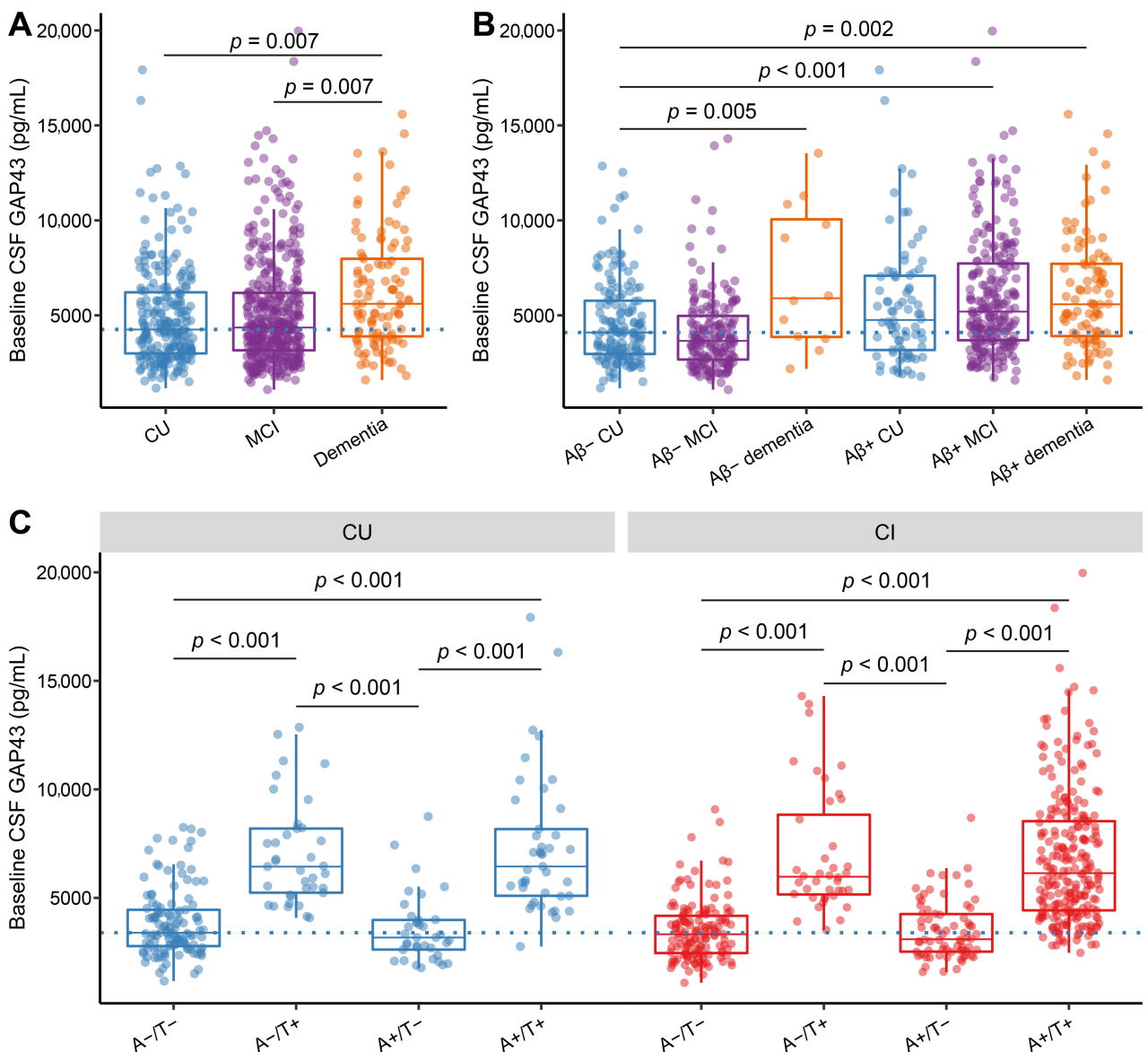


FIGURE 1: Comparison of baseline CSF GAP43 among different clinically- and biologically-defined stages of AD. Comparison of baseline CSF GAP43 among (A) different clinical diagnosis groups, (B) different A β positivity and clinical diagnosis groups, and (C) different A/T groups. The boxplots show the median (horizontal bar), interquartile range (IQR; hinges), and 1.5 \times IQR (whiskers). Each point represents an individual, and dashed lines represent the median values of the CU, A β - CU, or A-T- CU group. The p values of the comparisons are shown at the top, adjusting for age, sex, and APOE-ε4 status. Multiple comparisons correction was performed using the Benjamini-Hochberg method (FDR <0.05). The estimates of baseline CSF GAP43 in the CU group: A-T+ versus A-T- (estimate = 3,161 [95% CI 0.90–1.49], $p < 0.001$), A-T+ versus A+T- (estimate = 3,446 [95% CI 0.94–1.67], $p < 0.001$), A+T+ versus A-T- (estimate = 3,537 [95% CI 1.03–1.65], $p < 0.001$), A+T+ versus A+T- (estimate = 3,822 [95% CI 1.09–1.80], $p < 0.001$); The estimates of baseline CSF GAP43 in CI group: A-T+ versus A-T- (estimate = 3,557 [95% CI 0.92–1.50], $p < 0.001$), A-T+ versus A+T- (estimate = 3,601 [95% CI 0.91–1.55], $p < 0.001$), A+T+ versus A-T- (estimate = 3,221 [95% CI 0.90–1.29], $p < 0.001$), A+T+ versus A+T- (estimate = 3,265 [95% CI 0.89–1.33], $p < 0.001$). A = A β ; A β = β -amyloid; AD = Alzheimer's disease; CSF = cerebrospinal fluid; CU = cognitively unimpaired; FDR = false discovery rate; GAP43 = growth-associated protein-43; MCI = mild cognitive impairment; N = neurodegeneration; T = tau. [Color figure can be viewed at www.annalsofneurology.org]

GAP43 and longitudinal FDG PET was eliminated, which may result from the small number of individuals in each category.

Among 181 MCI individuals with a median (IQR) of 4.0 (2.0) years of follow-up clinical assessments, we found 136 remained stable (MCI-MCI), whereas

45 progressed to dementia (MCI-Dementia). The MCI-Dementia group had higher baseline CSF GAP43 (Fig 5A; estimate = 1,617 [95% CI 0.20–0.86], $p = 0.002$) and faster Δ CSF GAP43 increases (Fig 5B; estimate = 34 [95% CI 0.24–0.90], $p < 0.001$) than the MCI-MCI group. Additionally, the receiver operating

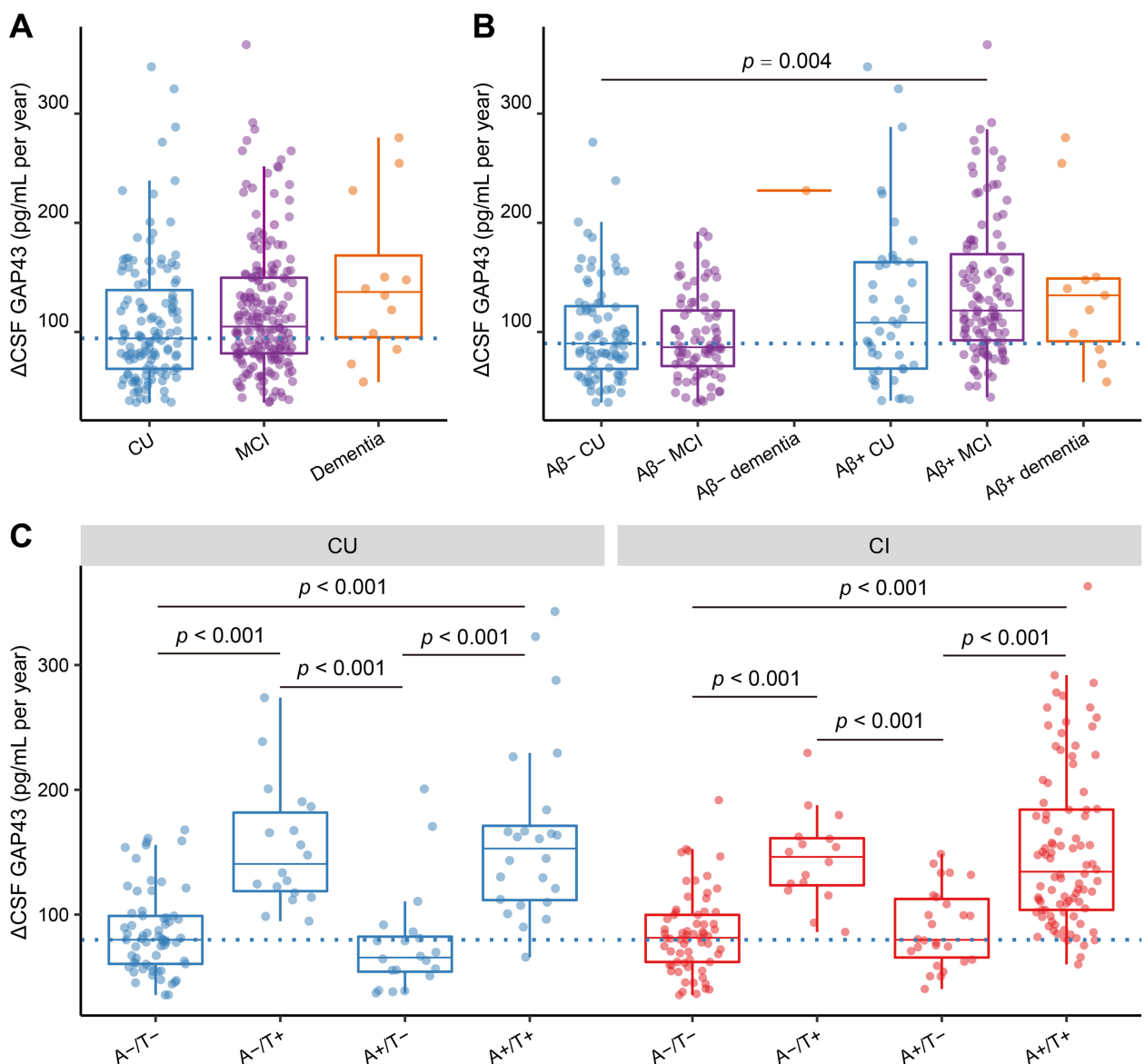


FIGURE 2: Comparison of longitudinal CSF GAP43 changes among different clinically- and biologically-defined stages of AD. Comparison of CSF GAP43 slopes (Δ CSF GAP43) among (A) different diagnosis groups, (B) different A β positivity and diagnosis groups, and (C) different A/T groups. The boxplots show the median (horizontal bar), interquartile range (IQR; hinges), and $1.5 \times$ IQR (whiskers). Each point represents an individual, and dashed lines represent the median values of the CU, A β - CU, or A-/T- CU group. The p values of the comparisons are shown at the top, adjusting for age, sex, and APOE-e4 status. Multiple comparisons correction was performed using the Benjamini-Hochberg method (FDR <0.05). The estimates of CSF GAP43 slopes in the CU group: A-/T + versus A-/T- (estimate = 69 [95% CI 0.75–1.60], p < 0.001), A-/T + versus A + /T- (estimate = 72 [95% CI 0.71–1.76], p < 0.001), A + /T + versus A-/T- (estimate = 85 [95% CI 1.03–1.87], p < 0.001), A + /T + versus A + /T- (estimate = 88 [95% CI 1.03–1.99], p < 0.001); The estimates of CSF GAP43 slopes in CI group: A-/T + versus A-/T- (estimate = 61 [95% CI 0.57–1.50], p < 0.001), A-/T + versus A + /T- (estimate = 62 [95% CI 0.51–1.58], p < 0.001), A + /T + versus A-/T- (estimate = 64 [95% CI 0.77–1.39], p < 0.001), A + /T + versus A + /T- (estimate = 64 [95% CI 0.72–1.45], p < 0.001). A = A β ; A β = β -amyloid; AD = Alzheimer's disease; CSF = cerebrospinal fluid; CU = cognitively unimpaired; FDR = false discovery rate; GAP43 = growth-associated protein-43; MCI = mild cognitive impairment; N = neurodegeneration; T = tau. [Color figure can be viewed at www.annalsofneurology.org]

characteristic analyses showed that baseline CSF GAP43 (Fig 5C; AUC = 0.704 [95% CI 0.61–0.79], sensitivity = 76.5%, specificity = 62.2%) and Δ CSF GAP43 (Fig 5D; AUC = 0.717 [95% CI 0.63–0.80], sensitivity = 68.1%, specificity = 71.1%) could significantly identify MCI progressors.

Mediation Analysis among Longitudinal CSF p-Tau₁₈₁, CSF GAP43, Hippocampal Volume, and Cognition

Among 326 individuals with longitudinal data, faster Δ CSF p-Tau₁₈₁ increases were negatively related to Δ rHCV ($\beta_{std} = -0.18$ [95% CI -0.28 to -0.07], p = 0.001) and

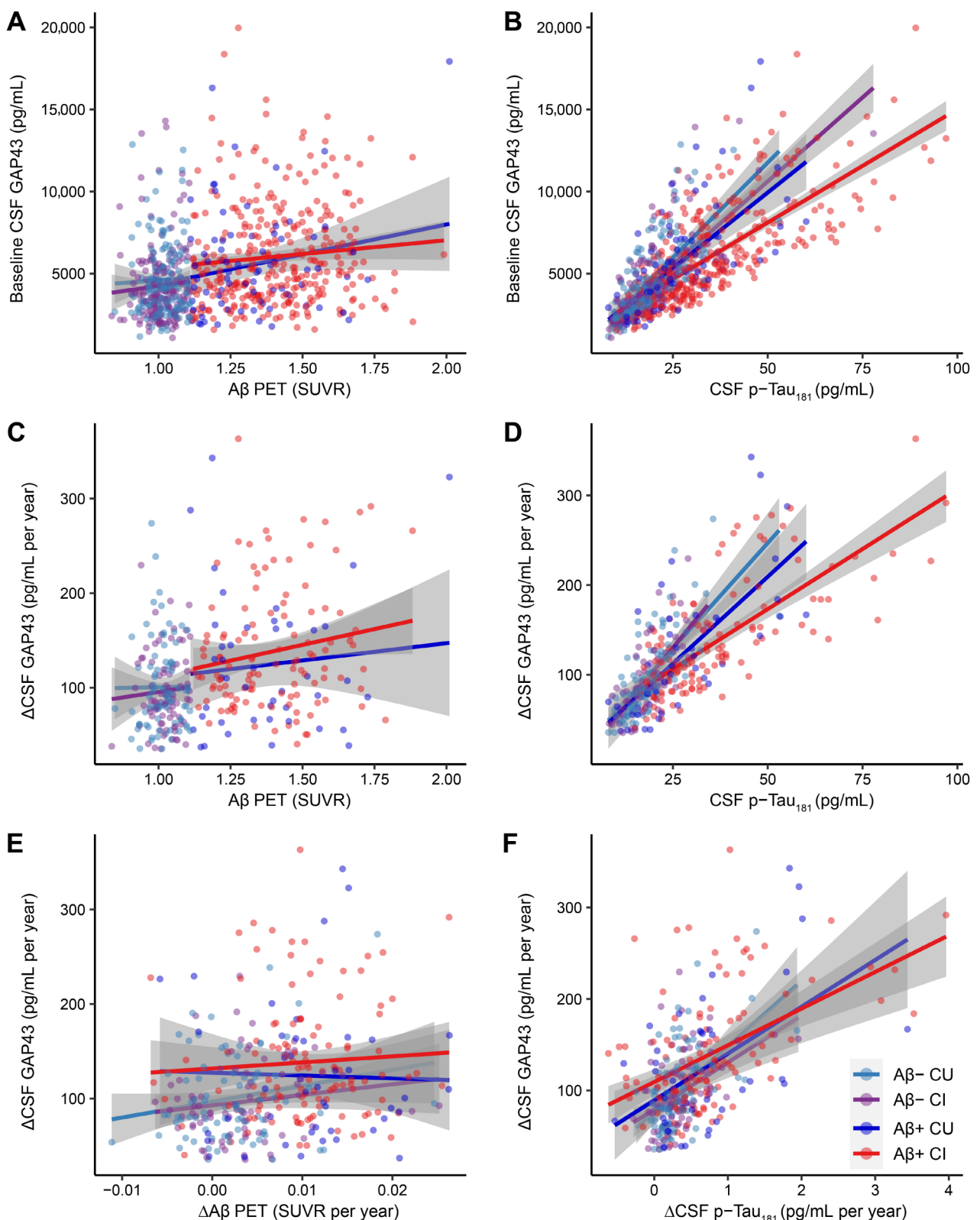


FIGURE 3: Association of CSF GAP43 with A β PET and CSF p-Tau in different A β PET and cognitive status. Associations of baseline CSF GAP43 with (A) baseline A β PET and (B) baseline CSF p-Tau₁₈₁. Associations of CSF GAP43 slopes (Δ CSF GAP43) with (C) baseline A β PET, (D) baseline CSF p-Tau₁₈₁, (E) A β PET slopes (Δ A β PET), and (F) CSF p-Tau₁₈₁ slopes (Δ CSF p-Tau₁₈₁). The points and solid lines represent each group's individuals and regression lines, adjusting for age, sex, and APOE- ϵ 4 status. A β = β -amyloid; CSF = cerebrospinal fluid; GAP43 = growth-associated protein-43; PET = positron emission tomography; p-Tau = phosphorylated tau. [Color figure can be viewed at www.annalsofneurology.org]

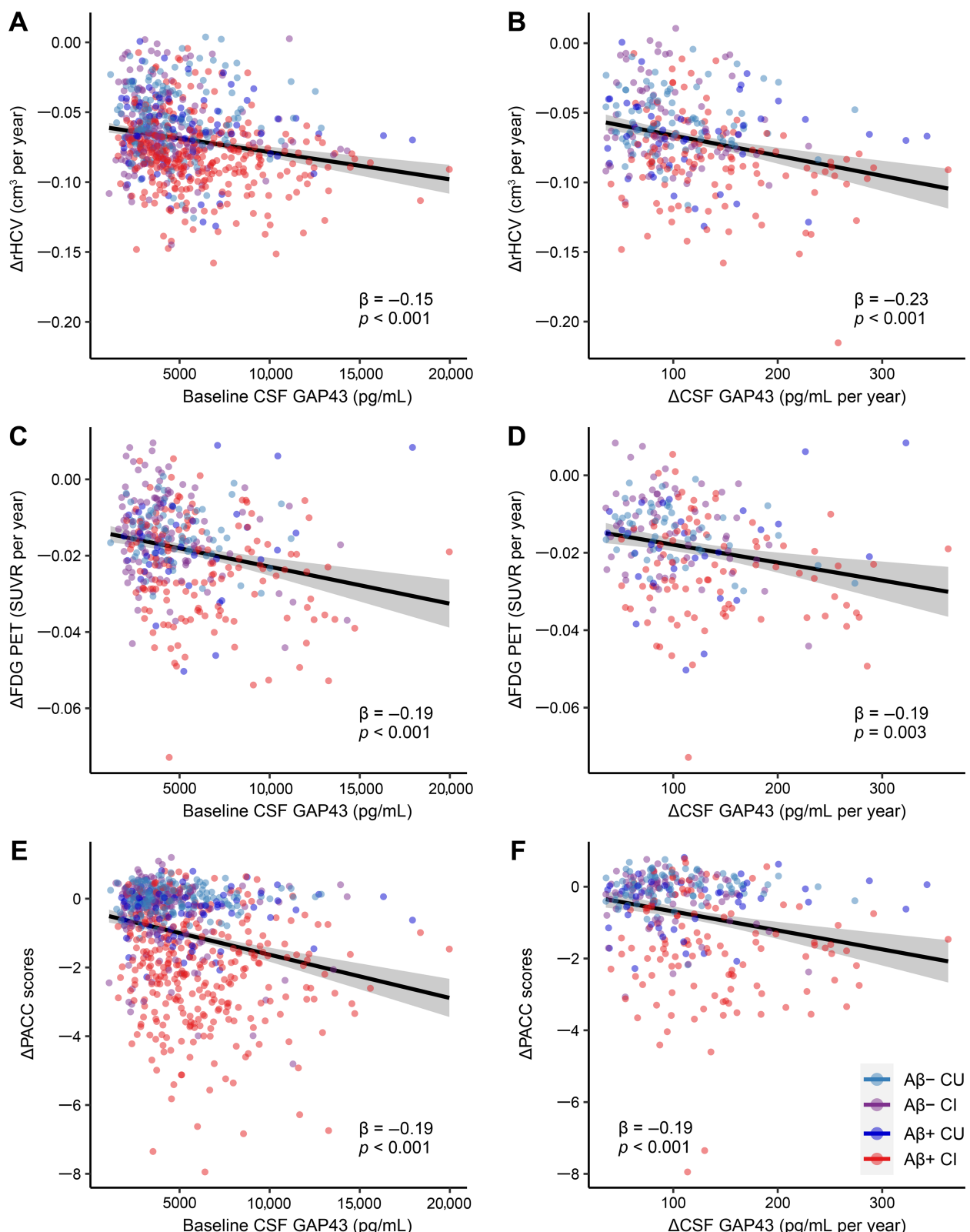


FIGURE 4: Association of CSF GAP43 with longitudinal neurodegeneration and cognitive decline. Associations of baseline CSF GAP43 with longitudinal changes of (A) rHCV (ΔrHCV), (C) FDG PET ($\Delta\text{FDG PET}$), and (E) PACC scores (ΔPACC scores). Associations of CSF GAP43 slope ($\Delta\text{CSF GAP43}$) with (B) ΔrHCV , (D) $\Delta\text{FDG PET}$, and (F) ΔPACC scores. The points and solid lines represent the individuals and regression lines, respectively. The standardized regression coefficients (β) and p values were computed using a linear model across all individuals, adjusting for age, sex, and APOE- $\epsilon 4$ status. CSF = cerebrospinal fluid; FDG = ^{18}F -fluorodeoxyglucose; GAP43 = growth-associated protein-43; PACC = preclinical Alzheimer cognitive composite; PET = positron emission tomography; rHCV = residual hippocampal volume [Color figure can be viewed at www.annalsofneurology.org]

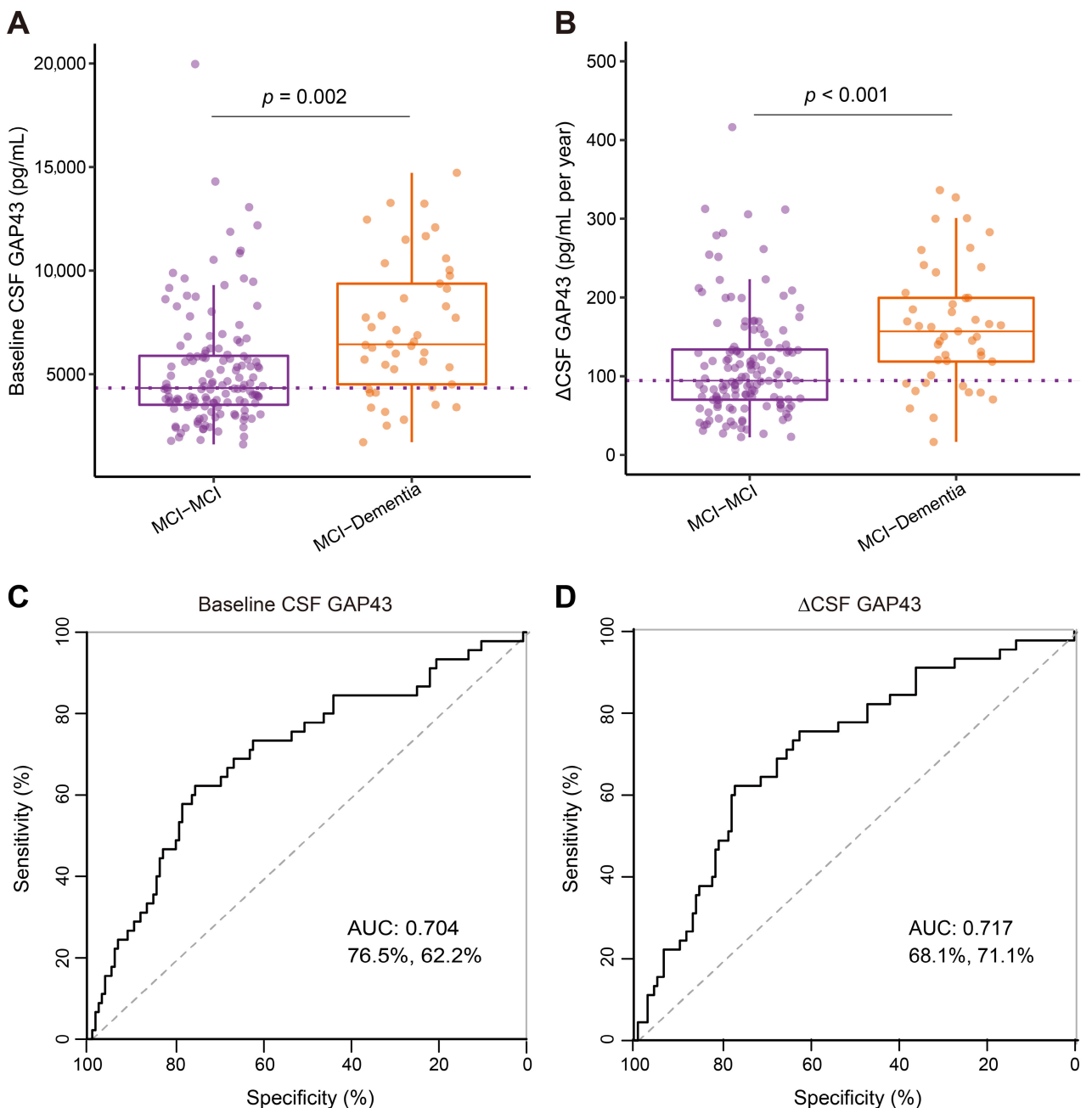


FIGURE 5: Association between CSF GAP43 and clinical progression of MCI patients. Comparison of (A) baseline CSF GAP43 and (B) slopes of CSF GAP43 (Δ CSF GAP43) between MCI-MCI and MCI-dementia patients. Receiver operating characteristic curve analysis for differentiating individuals with progressing MCI from those with stable MCI using (C) baseline CSF GAP43 and (D) Δ CSF GAP43. The boxplots show the median (horizontal bar), interquartile range (IQR; hinges), and $1.5 \times$ IQR (whiskers). The dots represent individual points of each group. The p values of the comparisons are shown at the top, adjusting for age, sex, and APOE- ϵ 4 status. Dashed lines represent the median values of the MCI-MCI patients. AUC = area under the curve; CSF = cerebrospinal fluid; GAP43 = growth-associated protein-43; MCI = mild cognitive impairment. [Color figure can be viewed at www.annalsofneurology.org]

Δ PACC scores ($\beta_{\text{std}} = -0.19$ [95% CI -0.30 to -0.09], $p < 0.001$). However, no significant association was found between Δ CSF p-Tau₁₈₁ and Δ FDG PET among 233 individuals with concurrent longitudinal CSF p-Tau₁₈₁ and FDG PET data ($\beta_{\text{std}} = -0.10$ [95% CI -0.23 to 0.03], $p = 0.116$). We further conducted a mediation analysis to determine the sequential associations among Δ CSF p-Tau₁₈₁

increases, Δ CSF GAP43 increases, Δ rHCV decreases, and Δ PACC decreases, and found that Δ CSF GAP43 and Δ rHCV significantly mediated the associations between Δ CSF p-Tau₁₈₁ and Δ PACC scores (Fig 6A), suggesting that tau-related presynaptic dysfunction is driving neurodegeneration and cognitive decline (Fig 6B). To strengthen the mediation effect in AD etiology, we re-ran the results using

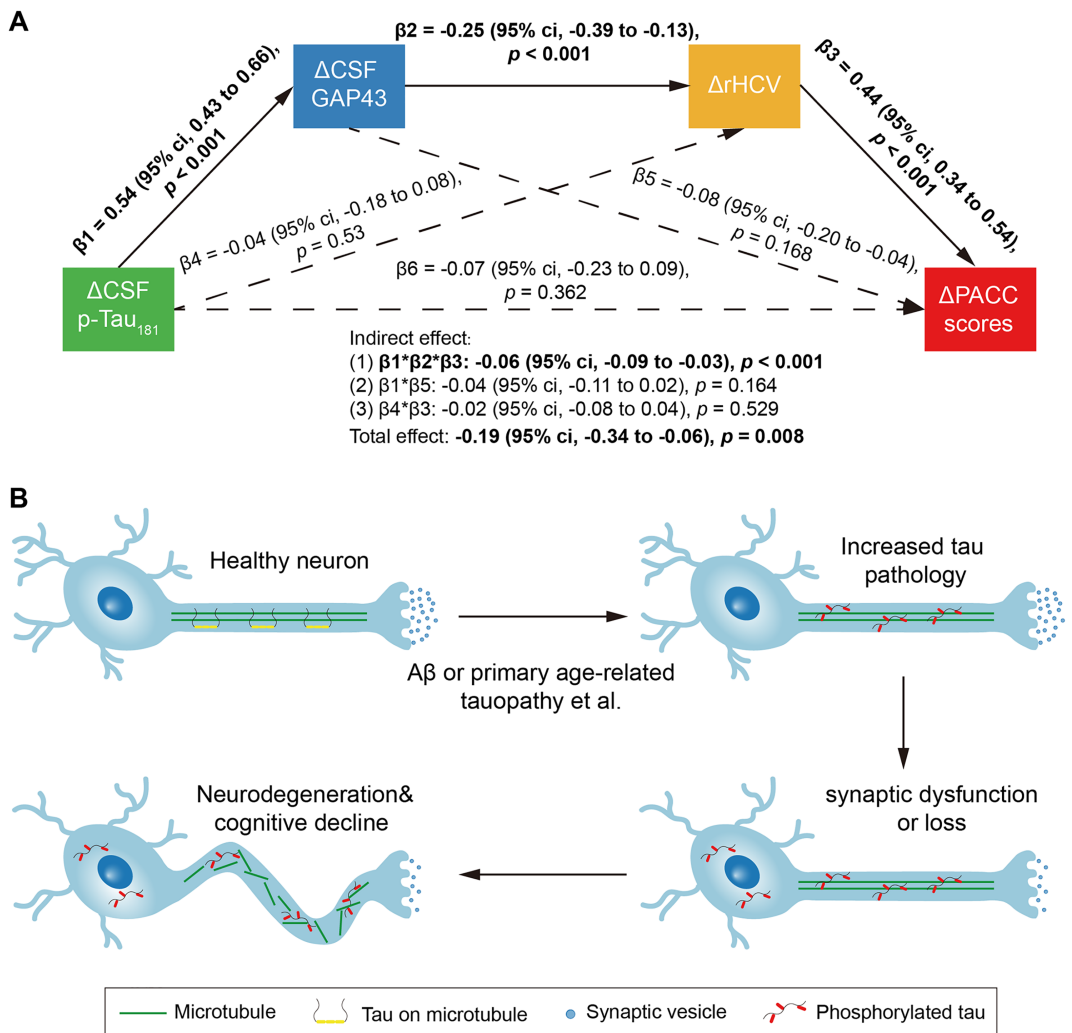


FIGURE 6: Sequential association among longitudinal changes of CSF p-Tau₁₈₁, CSF GAP43, hippocampal atrophy, and cognitive decline. (A) CSF GAP43 slope (Δ CSF GAP43) and hippocampal atrophy slope (Δ rHCV) fully mediated the association between CSF p-Tau₁₈₁ slope (Δ CSF p-Tau₁₈₁) and preclinical Alzheimer cognitive composite (PACC) score slope (Δ PACC). The solid and the dashed lines, respectively, show the significant and non-significant pathways. A 5,000-bootstrapping procedure computed total, direct, and indirect associations. **(B)** Schematic of the sequential cascade of tau aggregation, synaptic dysfunction, neurodegeneration, and cognitive decline in neurodegenerative disease. CSF = cerebrospinal fluid; GAP43 = growth-associated protein-43; p-Tau₁₈₁ = phosphorylated tau181. [Color figure can be viewed at www.annalsofneurology.org]

the same mediation analysis when A β - CI participants were excluded from our model. The outcomes were largely the same.

Discussion

In this study, we investigated the alterations of CSF GAP43 in different clinical and biological stages of AD, and how they relate to A β , tau, neurodegeneration, and cognitive decline cross-sectionally and longitudinally. CSF p-Tau₁₈₁-positive individuals showed higher CSF GAP43 concentrations and faster rates of CSF GAP43 increases than CSF p-Tau₁₈₁-negative individuals regardless of A β positivity and cognitive status. Multivariate regression analyses extended these findings by showing that CSF

GAP43 correlated positively with the CSF p-Tau₁₈₁ in both cross-sectional and longitudinal cohorts, independent of the A β PET profile. Furthermore, the longitudinal MRI and cognition data revealed that higher CSF GAP43 concentrations and faster rates of CSF GAP43 increases were associated with longitudinal decreases in hippocampal volume, glucose metabolism, and cognition. Finally, the mediation analyses demonstrated that more rapid rates of GAP43 increases significantly mediated the longitudinal associations among CSF p-Tau₁₈₁, hippocampal atrophy, and cognitive decline. Altogether, these findings suggest that elevated tau pathology rather than A β plaque is closely related to presynaptic dysfunction measured by CSF GAP43, which can lead to subsequent neurodegeneration and cognitive decline.

In line with the present findings, previous cross-sectional studies reported higher CSF GAP43 concentrations in patients with MCI^{24, 34} or dementia²² compared with the CU individuals. However, they did not stratify participants by A β status nor did they investigate longitudinal changes of CSF GAP43. We found higher CSF GAP43 concentrations in A β - dementia, A β + MCI, and A β + dementia groups than in the A β - CU group. Longitudinally, we observed significantly faster CSF GAP43 increases in A β + MCI individuals than in the A β - CU controls. We also observed marginally higher CSF GAP43 concentrations in A β + CU individuals, in accordance with the results reported by two recent cross-sectional studies.^{34, 35} Together, CSF GAP43 may likely increase in both symptomatic AD patients and people with suspected non-AD dementia.

Among different biological stages of AD, we found that CSF p-Tau₁₈₁-positive individuals (A-/T+ or A+/T+) had both higher CSF GAP43 concentrations and faster rates of CSF GAP43 increases compared with the A-/T- or A+/T- individuals, regardless of clinical status. One recent study reported that tau-positive MCI patients had higher CSF GAP43 concentrations than the tau-negative MCI patients, which was in accordance with the present results.²⁴ However, another recently important study found elevated CSF GAP43 concentrations in A+/T- individuals than in the A-/T- individuals.²⁵ Notably, they defined abnormal tau positivity using tau PET imaging, which may be a relatively later biomarker of the formation of tau aggregation than CSF p-Tau according to previous reports by our group⁵ and other laboratories.^{36, 37} Importantly, the multivariate regression analyses in the present study provide further evidence for explaining that CSF GAP43 increases were positively associated with tau pathology rather than A β plaques in both cross-sectional and longitudinal analyses, regardless of A β positivity and cognitive status. In contrast, two cross-sectional studies found CSF GAP43 was associated with A β and tau pathologies, but they did not analyze their independent effect.^{22, 23} Recently, another two cross-sectional studies reported no association between A β pathology and CSF GAP43 when controlling for CSF p-Tau,^{24, 35} supporting the findings in the present study. Together with our results and previous literature, the presynaptic dysfunction measured by CSF GAP43 may be closely linked to tau pathology independent of cortical A β deposition and clinical diagnosis.

The substantial synaptic loss may contribute to neurodegeneration in the brain, leading to cognitive impairment.^{15, 38, 39} Thus, we subsequently explored the predictive effects of CSF GAP43 on longitudinal hippocampal atrophy, hypometabolism, and cognitive decline.

This showed that CSF GAP43 was associated with more rapid hippocampal atrophy and cognitive decline, especially in symptomatic AD, as well as hypometabolism. Additionally, in a subgroup of MCI patients with follow-up clinical assessments, we found that higher CSF GAP43 concentrations and faster rates of CSF GAP43 increases could identify progressing MCI individuals with >70% AUC values. Consistent with the present findings, higher CSF GAP43 concentrations were reported to be negatively associated with cortical thickness³⁵ and cognition.²² However, in contrast to the present study, one cross-sectional study found elevated CSF GAP43 concentrations were weakly related to higher glucose metabolism, which may be explained by the fact that they focused on preclinical AD individuals.³⁵ Notably, previous studies^{40, 41} showed that brain metabolism hyperactivity appeared to be detected in some brain regions in the early stage of AD, which could be driven by activated microglial.⁴² Previous studies reported that CSF p-Tau was significantly related to neurodegeneration and cognitive decline.⁴³⁻⁴⁵ Intriguingly, our mediation analysis provided further novel findings that presynaptic dysfunction measured by CSF GAP43 fully mediated the associations of CSF p-Tau₁₈₁ increases with longitudinal hippocampal atrophy and cognitive decline.

Given the close relationship between synaptic function and cognition, the very early response of presynapse to pathological tau changes emphasizes the importance of therapeutic strategies targeting tau pathology at the pre-symptomatic stage in clinical trials, which may contribute to diminishing synaptic impairment and ameliorating cognition. Furthermore, the present results suggest that CSF GAP43 could be used as an indirect biomarker of presynapse for evaluating the progression of synaptic pathology in patients and monitoring the exacerbation of neurodegenerative dementia in clinical practice. Despite the annual changes of CSF GAP43 being gentle and consistent with previous longitudinal studies of other CSF biomarkers, we found that more rapid increases in CSF GAP43 were related to faster hippocampal atrophy, hypometabolism, and cognitive decline.^{46, 47} Nonetheless, additional longitudinal studies based on different cohorts are critical to confirm the longitudinal changes in CSF GAP43.

In the present study, we used a large dataset to explore the abnormal changes of presynaptic protein measured by CSF GAP43 among different stages of AD, and how presynaptic loss relates to A β plaques, CSF p-Tau₁₈₁, hippocampal atrophy, hypometabolism, and cognitive decline. These findings might provide novel insights into understanding the role of presynaptic loss in AD, and extend current A/T/N biomarkers to detect neurodegenerative diseases.

However, this study had some limitations, as follows. We selected CSF p-Tau₁₈₁ to represent tau pathology, which may be inferior to other phosphorylation sites (such as p-Tau₂₁₇,^{48, 49} which is not available in ADNI), and these findings still require further investigation in tau PET imaging.⁵⁰ Although CSF GAP43 was related to tau pathology measured by CSF p-Tau₁₈₁, the current study is correlational in nature and does not test CSF p-Tau₁₈₁ or CSF GAP43 changes as a causal event. All we can confirm is that there seems to be an association with processes that result in elevated CSF p-Tau₁₈₁ and GAP43. Autopsy confirmation would be required in the future. In addition, this cohort lacks other synapse-related biomarkers (such as presynaptic protein SNAP-25 and postsynaptic protein neurogranin, whose sample sizes in the ADNI cohort are limited), which may reflect the different mechanism of synapse degeneration occurring in various stages of the disease. Additional confirmation is still required by using other synaptic proteins. Finally, the longitudinal data of CSF GAP43 and FDG PET were limited, which may need to be validated by further longitudinal data with more visits and longer follow-up periods.

In conclusion, the present study provides novel insights into the association of presynaptic loss with A β , tau, neurodegeneration, and cognitive decline, where elevated tau pathology is driving presynaptic dysfunction or loss, resulting in subsequent neurodegeneration and cognitive decline. The tau-related presynaptic protein, GAP43, in CSF may be a promising biomarker for synaptic damage. It can strengthen the measurement of neurodegeneration beyond the current commonly-used neurodegeneration biomarkers, which may provide more information to understand the characteristics and progression of neurodegenerative diseases.

Acknowledgments

This work was supported by the National Natural Science Foundation of China (82171197), the Shenzhen Bay Laboratory Key Project (S211101002-2), and the Shenzhen Bay Laboratory Open Project (SZBL2020090501014).

The authors thank all the ADNI participants and staff for their contributions to data acquisition. The Data collection and sharing for this project were funded by the ADNI (National Institutes of Health Grant U01 AG024904) and DOD ADNI (Department of Defense award number W81XWH-12-2-0012). ADNI is funded by the National Institute on Aging, the National Institute of Biomedical Imaging and Bioengineering, and through generous contributions from the following: AbbVie, Alzheimer's Association; Alzheimer's Drug Discovery Foundation; Araclon Biotech; BioClinica, Inc.; Biogen;

Bristol-Myers Squibb Company; CereSpir, Inc.; Eisai Inc.; Elan Pharmaceuticals, Inc.; Eli Lilly and Company; EuroImmun; F. Hoffmann-La Roche Ltd and its affiliated company Genentech, Inc.; Fujirebio; GE Healthcare; IXICO Ltd.; Janssen Alzheimer Immunotherapy Research & Development, LLC.; Johnson & Johnson Pharmaceutical Research & Development LLC.; Lumosity; Lundbeck; Merck & Co., Inc.; Meso Scale Diagnostics, LLC.; NeuroRx Research; Neurotrack Technologies; Novartis Pharmaceuticals Corporation; Pfizer Inc.; Piramal Imaging; Servier; Takeda Pharmaceutical Company; and Transition Therapeutics. The Canadian Institutes of Health Research is providing funds to support ADNI clinical sites in Canada. Private sector contributions are facilitated by the Foundation for the National Institutes of Health (www.nih.gov). The grantee organization is the Northern California Institute for Research and Education, and the study is coordinated by the Alzheimer's Disease Cooperative Study at the University of California, San Diego. ADNI data are disseminated by the Laboratory for Neuro Imaging at the University of Southern California.

Author Contributions

T.G. and G.L. contributed to the conception and design of the study; T.G., G.L., Y.C., and A.L. contributed to the acquisition and analysis of data; T.G., G.L., Z.L., and S.M. contributed to drafting the manuscript and preparing the figures.

Potential Conflicts of Interest

Nothing to report.

Data Availability

All data used in the current study were obtained from the ADNI database (available at <https://adni.loni.usc.edu>). Derived data are available from the corresponding author on request by any qualified investigator subject to a data use agreement.

References

1. Jagust W. Imaging the evolution and pathophysiology of Alzheimer disease. *Nat Rev Neurosci* 2018;19:687–700.
2. Guo T, Brendel M, Grimmer T, et al. Predicting regional pattern of longitudinal β -amyloid accumulation by baseline PET. *J Nucl Med* 2017;58:639–645.
3. Schöll M, Lockhart SN, Schonhaut DR, et al. PET imaging of tau deposition in the aging human brain. *Neuron* 2016;89:971–982.
4. Guo T, Shaw LM, Trojanowski JQ, et al. Association of CSF A β , amyloid PET, and cognition in cognitively unimpaired elderly adults. *Neurology* 2020;95:e2075–e2085.

5. Guo T, Korman D, La Joie R, et al. Normalization of CSF pTau measurement by A β 40 improves its performance as a biomarker of Alzheimer's disease. *Alzheimer's Res Ther* 2020;12:97.
6. Jack CR, Bennett DA, Blennow K, et al. NIA-AA research framework: toward a biological definition of Alzheimer's disease. *Alzheimers Dement* 2018;14:535–562.
7. Jack CR, Wiste HJ, Therneau TM, et al. Associations of amyloid, tau, and neurodegeneration biomarker profiles with rates of memory decline among individuals without dementia. *JAMA* 2019;321:2316–2325.
8. Guo T, Korman D, Baker SL, et al. Longitudinal cognitive and biomarker measurements support a unidirectional pathway in Alzheimer's disease pathophysiology. *Biol Psychiatry* 2021;89:786–794.
9. Dodich A, Mendes A, Assal F, et al. The A/T/N model applied through imaging biomarkers in a memory clinic. *Eur J Nucl Med Mol Imaging* 2020;47:247–255.
10. Ebenau JL, Timmers T, Wesselman LMP, et al. ATN classification and clinical progression in subjective cognitive decline. *Neurology* 2020;95:e46–e58.
11. Altomare D, de Wilde A, Ossenkoppele R, et al. Applying the ATN scheme in a memory clinic population: the ABIDE project. *Neurology* 2019;93:e1635–e1646.
12. Burke BT, Latimer C, Keene CD, et al. Theoretical impact of the AT(N) framework on dementia using a community autopsy sample. *Alzheimers Dement* 2021;17:1879–1891.
13. Ingala S, De Boer C, Masselink LA, et al. Application of the ATN classification scheme in a population without dementia: findings from the EPAD cohort. *Alzheimers Dement* 2021;17:1189–1204.
14. Hampel H, Cummings J, Blennow K, et al. Developing the ATX(N) classification for use across the Alzheimer disease continuum. *Nat Rev Neurol* 2021;17:580–589.
15. Chen Y, Fu AKY, Ip NY. Synaptic dysfunction in Alzheimer's disease: mechanisms and therapeutic strategies. *Pharmacol Ther* 2019;195:186–198.
16. De Wilde MC, Overk CR, Sijben JW, Masliah E. Meta-analysis of synaptic pathology in Alzheimer's disease reveals selective molecular vesicular machinery vulnerability. *Alzheimers Dement* 2016;12:633–644.
17. Forner S, Baglietto-Vargas D, Martini AC, et al. Synaptic impairment in Alzheimer's disease: a dysregulated symphony. *Trends Neurosci* 2017;40:347–357.
18. Neve RL, Finch EA, Bird ED, Benowitz LI. Growth-associated protein GAP-43 is expressed selectively in associative regions of the adult human brain. *Proc Natl Acad Sci* 1988;85:3638–3642.
19. Benowitz L, Perrone-Bizzozero N, Finklestein S, Bird E. Localization of the growth-associated phosphoprotein GAP-43 (B-50, F1) in the human cerebral cortex. *J Neurosci* 1989;9:990–995.
20. Davidsson P, Blennow K. Neurochemical dissection of synaptic pathology in Alzheimer's disease. *Int Psychogeriatr* 1998;10:11–23.
21. Bogdanovic N, Davidsson P, Volkmann I, et al. Growth-associated protein GAP-43 in the frontal cortex and in the hippocampus in Alzheimer's disease: an immunohistochemical and quantitative study. 2000.
22. Sandelin Å, Portelius E, Källén Å, et al. Elevated CSF GAP-43 is Alzheimer's disease specific and associated with tau and amyloid pathology. *Alzheimers Dement* 2019;15:55–64.
23. Tible M, Sandelin Å, Höglund K, et al. Dissection of synaptic pathways through the CSF biomarkers for predicting Alzheimer disease. *Neurology* 2020;95:e953–e961.
24. Bergström S, Remnäst J, Yousef J, et al. Multi-cohort profiling reveals elevated CSF levels of brain-enriched proteins in Alzheimer's disease. *Ann Clin Transl Neurol* 2021;8:1456–1470.
25. Pereira JB, Janelidze S, Ossenkoppele R, et al. Untangling the association of amyloid- β and tau with synaptic and axonal loss in Alzheimer's disease. *Brain* 2021;144:310–324.
26. Hansson O, Seibyl J, Stomrud E, et al. CSF biomarkers of Alzheimer's disease concord with amyloid- β PET and predict clinical progression: a study of fully automated immunoassays in BioFINDER and ADNI cohorts. *Alzheimers Dement* 2018;14:1470–1481.
27. Desikan RS, Ségonne F, Fischl B, et al. An automated labeling system for subdividing the human cerebral cortex on MRI scans into gyral based regions of interest. *Neuroimage* 2006;31:968–980.
28. Landau SM, Fero A, Baker SL, et al. Measurement of longitudinal β -amyloid change with 18 F-Florbetapir PET and standardized uptake value ratios. *J Nucl Med* 2015;56:567–574.
29. Landau SM, Mintun MA, Joshi AD, et al. Amyloid deposition, hypometabolism, and longitudinal cognitive decline. *Ann Neurol* 2012;72:578–586.
30. Jack CR, Knopman DS, Weigand SD, et al. An operational approach to National Institute on Aging-Alzheimer's Association criteria for preclinical Alzheimer disease. *Ann Neurol* 2012;71:765–775.
31. Schindler SE, Gray JD, Gordon BA, et al. Cerebrospinal fluid biomarkers measured by Elecsys assays compared to amyloid imaging. *Alzheimers Dement* 2018;14:1460–1469.
32. Donohue MC, Sperling RA, Salmon DP, et al. The preclinical Alzheimer cognitive composite: measuring amyloid-related decline. *JAMA Neurol* 2014;71:961–970.
33. Rosseel Y. Lavaan: an R package for structural equation modeling. *J Stat Softw* 2012;48:1–93.
34. Remnäst J, Just D, Mitsios N, et al. CSF profiling of the human brain enriched proteome reveals associations of neuromodulin and neurogranin to Alzheimer's disease. *Proteomics* 2016;10:1242–1253.
35. Milà-Alomà M, Brinkmalm A, Ashton NJ, et al. CSF synaptic biomarkers in the preclinical stage of Alzheimer disease and their association with MRI and PET: a cross-sectional study. *Neurology* 2021;97:e2065–e2078. <https://doi.org/10.1212/WNL.00000000000012853>.
36. Meyer P-F, Pichet Binette A, Goncalves J, et al. Characterization of Alzheimer disease biomarker discrepancies using cerebrospinal fluid phosphorylated tau and AV1451 positron emission tomography. *JAMA Neurol* 2020;77:508–516.
37. Mattsson-Carlsgren N, Andersson E, Janelidze S, et al. A β deposition is associated with increases in soluble and phosphorylated tau that precede a positive tau PET in Alzheimer's disease. *Sci Adv* 2020;6:eaaz2387.
38. Terry RD, Masliah E, Salmon DP, et al. Physical basis of cognitive alterations in Alzheimer's disease: synapse loss is the major correlate of cognitive impairment 1991.
39. Jacobs J, Kahana MJ. Direct brain recordings fuel advances in cognitive electrophysiology. *Trends Cogn Sci* 2010;14:162–171.
40. Johnson SC, Christian BT, Okonkwo OC, et al. Amyloid burden and neural function in people at risk for Alzheimer's disease. *Neurobiol Aging* 2014;35:576–584.
41. Oh H, Habeck C, Madison C, Jagust W. Covarying alterations in A β deposition, glucose metabolism, and gray matter volume in cognitively normal elderly. *Hum Brain Mapp* 2014;35:297–308.
42. Xiang X, Wind K, Wiedemann T, et al. Microglial activation states drive glucose uptake and FDG-PET alterations in neurodegenerative diseases. *Sci Transl Med* 2021;13:eabe5640.
43. Barthélémy NR, Li Y, Joseph-Mathurin N, et al. A soluble phosphorylated tau signature links tau, amyloid and the evolution of stages of dominantly inherited Alzheimer's disease. *Nat Med* 2020;26:398–407.
44. Llibre-Guerra JJ, Li Y, Schindler SE, et al. Association of Longitudinal Changes in cerebrospinal fluid Total tau and phosphorylated tau 181 and brain atrophy with disease

- progression in patients with Alzheimer disease. *JAMA Netw Open* 2019;2:e1917126.
45. Pascoal TA, Mathotaarachchi S, Shin M, et al. Synergistic interaction between amyloid and tau predicts the progression to dementia. *Alzheimers Dement* 2017;13:644–653.
46. Kester MI, Teunissen CE, Crimmins DL, et al. Neurogranin as a cerebrospinal fluid biomarker for synaptic loss in symptomatic Alzheimer disease. *JAMA Neurol* 2015;72:1275–1280.
47. Lleó A, Alcolea D, Martínez-Lage P, et al. Longitudinal cerebrospinal fluid biomarker trajectories along the Alzheimer's disease continuum in the BIOMARKAPD study. *Alzheimers Dement* 2019;15:742–753.
48. Janelidze S, Stomrud E, Smith R, et al. Cerebrospinal fluid p-tau217 performs better than p-tau181 as a biomarker of Alzheimer's disease. *Nat Commun* 2020;11:1683.
49. Leuzy A, Janelidze S, Mattsson-Carlgren N, et al. Comparing the clinical utility and diagnostic performance of cerebrospinal fluid P-Tau181, P-Tau217 and P-Tau231 assays. *Neurology* 2021;97:e1681–e1694. <https://doi.org/10.1212/WNL.00000000000012727>.
50. Ossenkoppele R, Reimand J, Smith R, et al. Tau PET correlates with different Alzheimer's disease-related features compared to CSF and plasma p-tau biomarkers. *EMBO Mol Med* 2021;13:1–15.